

Polyatomic Liquid Oxygen (PLO[®]): A new methodology for the production in aqueous solution of reactive oxygen and nitrogen species (RONS) to be applied in medical treatments

Cite as: AIP Advances **11**, 125218 (2021); <https://doi.org/10.1063/5.0075895>

Submitted: 19 October 2021 • Accepted: 25 November 2021 • Published Online: 16 December 2021

Giovanni Barco,  Emilia Bramanti,  Massimo Onor, et al.

COLLECTIONS

Paper published as part of the special topic on [Biophysics and Bioengineering](#)



View Online



Export Citation



CrossMark

ARTICLES YOU MAY BE INTERESTED IN

[Hemoglobin estimation using ultra-low path length in microfluidic chips by quantifying Soret band](#)

AIP Advances **11**, 075323 (2021); <https://doi.org/10.1063/5.0057490>

[A 3D passive micromixer with particle of stochastic motion through limonene dissolution method](#)

AIP Advances **11**, 105318 (2021); <https://doi.org/10.1063/5.0067135>

[Wireless power transfer in attenuating media](#)

AIP Advances **11**, 115303 (2021); <https://doi.org/10.1063/5.0059932>



Call For Papers!

AIP Advances

SPECIAL TOPIC: Advances in Low Dimensional and 2D Materials

Polyatomic Liquid Oxygen (PLO[®]): A new methodology for the production in aqueous solution of reactive oxygen and nitrogen species (RONS) to be applied in medical treatments

Cite as: AIP Advances 11, 125218 (2021); doi: 10.1063/5.0075895

Submitted: 19 October 2021 • Accepted: 25 November 2021 •

Published Online: 16 December 2021



View Online



Export Citation



CrossMark

Giovanni Barco,^{1,a)} Emilia Bramanti,²  Massimo Onor,²  Edoardo Benedetti,³ Marina Mameli,¹ Andrea Mangano,^{4,b)} Alessandro Pascone,^{4,c)}  and Ubaldo Prati^{1,d)} 

AFFILIATIONS

¹ Istituto Internazionale Barco, Ricerche e Cure Ossidative, Pisa 56121, Italy

² National Research Council of Italy, C.N.R., Institute of Chemistry of Organo Metallic Compounds-ICCOM, Pisa 56124, Italy

³ Azienda Ospedaliero Universitaria Pisana, Hematology Unit, Department of Oncology, University of Pisa, Pisa 56126, Italy

⁴ ASPHE Biotech Srl, Milano 20149, Italy

^{a)} giovanni.barco@libero.it

^{b)} dir.ricerca.sviluppo@asphe-biotech.it

^{c)} alexpascone@gmail.com

^{d)} Author to whom correspondence should be addressed: prati.u@libero.it

ABSTRACT

Free radicals play a pivotal role in cell physiology as “gaseous messengers/transmitters.” The radical superoxide ($O_2^{\cdot-}$) and H_2O_2 molecules are called Reactive Oxygen Species (ROS); nitric oxide and peroxyxynitrite are named Reactive Nitrogen Species (RNS). All these species constitute an integrated cellular signaling system. ROS and RNS act on cell proliferation, differentiation, migration, and apoptosis, thus becoming potential anticancer drugs. Because of their chemical instability and short half-life, they cannot be used directly. In this work, we describe an original methodology to produce an aqueous mixture of reactive oxygen and nitrogen species (RONS) in which the gas transmitter molecules derived from the dioxygen and nitrogen oxide have sufficient chemical stability, suitable for *in vitro* studies of cell physiology. This technique is based on the generation of an electron beam obtained through an inverse sputtering electron device. The result is a gaseous mixture of allotropes of both oxygen and nitrogen in trace amounts, later dissolved in an aqueous phase. This mixture is defined either with the acronym OPL[®] (Ossigeno Poliatomico Liquido) or PLO[®] (Polyatomic Liquid Oxygen) or OPL-RONS[®]. We report herein the chemical characterization of PLO. The stability of PLO makes it suitable for *in vivo* studies and medical applications.

© 2021 Author(s). All article content, except where otherwise noted, is licensed under a Creative Commons Attribution (CC BY) license (<http://creativecommons.org/licenses/by/4.0/>). <https://doi.org/10.1063/5.0075895>

I. INTRODUCTION

Free radicals are highly reactive chemical species, and for this reason, they are characterized by a very short half-life. They are made up of several atoms or just one atom with unpaired electronic arrangement that makes them extremely reactive.

The Reactive Oxygen Species (ROS) are characterized by a strong oxidative capacity, greater than the molecular oxygen, which in water shows a redox potential of -0.16 V. The higher the charge/volume ratio, the more reactive are ROS and the shorter

their half-life is. Moreover, half-life can be further reduced by pH, temperature, and the presence of contaminants.

Many observations of cell physiology have highlighted the importance of radicals, i.e., molecules with only one non-coupled electron and therefore called one-electron oxidant. Radicals have different reduction potentials. For example, the hydroxyl radical (OH^{\cdot}) has a large reduction potential of 2.31 V (pH 7), while molecular oxygen (O_2) shows a potential of -0.16 V, the weak oxidative activity essential for an efficient mitochondrial function. Molecular oxygen is the last electron acceptor in the final part of oxidative

phosphorylation due to its favorable reduction potential compared to water.

The radicals, for their important cellular physiological role, are included in the group of “gaseous messengers/transmitters,”²¹ a group of small gaseous molecules known for their high toxicity. They are generated in the cells and are effectors of important physiological actions. Some of these gaseous transmitter molecules, such as superoxide ($O_2^{\cdot-}$) and H_2O_2 , which can act as cellular signaling agents, come from molecular oxygen (O_2), while other species come from nitric oxide (NO).^{2,3} Other species, such as carbon monoxide (CO) and hydrogen sulfide (H_2S), are toxic. The radical superoxide ($O_2^{\cdot-}$) and H_2O_2 molecules are called *Reactive Oxygen Species (ROS)*; nitric oxide (NO) and peroxyxynitrite ($ONOO^-$)⁴ are named *Reactive Nitrogen Species (RNS)*. All these species constitute an actual integrated cellular signaling system.

ROS and RNS act on cell proliferation, differentiation, migration, and apoptosis, thus becoming potential anticancer drugs.

Gas transmitters act only when they are dissolved in biological fluids. Because of their chemical instability and short half-life, they cannot be used directly,⁵ and their production and *in vitro* study are not trivial. Recent studies have overcome the problem by using titanium dioxide nanoparticles that, once suitably stimulated, locally release ROS with antineoplastic activity.⁶

In the last 20 years, this research group studied the production of a sterile aqueous ROS solution to be used for scientific and therapeutic purposes.⁷ The first device produced an allotropic mixture of oxygen and the ROS contained in the mixture delivered in bi-distilled water through an ion-exchange semipermeable membrane. However, the system did not allow us to obtain constant quantity and the type of ROS for the time necessary for their scientific or medical use. In 2017, based on past experiences, we developed a new system that allows a stable production of reactive oxygen and nitrogen species (RONS) (ROS + RNS).^{8–10} The method allows us to obtain different types of RONS aqueous mixtures with different concentrations of radicals depending on the needs, which we indicate with the acronym OPL[®] (Ossigeno Poliatomico Liquido) or PLO[®] (Polyatomic Liquid Oxygen).

This study describes this new methodology to produce ROS and RNS, and their chemical characterization in aqueous solution. The RONS mixtures had a suitable stability for *in vitro* studies and for possible medical applications.

II. MATERIALS AND METHODS

A. Generation of PLO

The PLO generation system is based on DME, a device developed by Istituto Internazionale Barco, working with an oxygen/nitrogen source and other associated products as shown in Fig. 1(a).

The system allows and controls the generation of an allotropic mixture and RONS (highly reactive oxygen and nitrogen species). Within the inverse sputtering electron generator,¹⁰ the emission of electrons by the thallium cathode⁸ occurs when the gaseous mixture is introduced into the sputtering chamber. Depending on the percentages of allotropes of oxygen and/or nitrogen introduced into the ionization chamber, different types of OPL with different concentrations of ROS or RNS may be generated. The inverse sputtering electron device, which is conventionally used to hit target materials

with positive ions, has been modified to hit the gaseous mixture with released *sputtering electrons*. The oxygen concentrator is a medical device, EverFlo[™] by Respiration Deutch, by Philips, which produces concentrated oxygen from room air. The oxygen from the air is concentrated using a molecular sieve and a pressure swing adsorption process. However, the PLO generator system is also compatible with a cylinder containing medical oxygen equipped with a pressure switch to regulate the entry pressure of medical oxygen into the DME. The adduction kit, model 1000130/1000169 by Emotec, is the circuit where the phase transformation of oxygen takes place from medical gas to stable liquid, thanks to the supply of medicinal water from an external tank, becoming OPL.

Oxygen atoms are defined as “degenerate” because they are characterized by two unpaired electrons with parallel spin, positioned on two different orbitals (π^*2p). These species undergo reductive phenomena, accepting sputtering electrons and forming ROS and RNS. There are different types of plasma sputtering devices, and the diode technology types are the more suited for production of ROS. It is important to underline that during the sputtering process, the relaxation of the excited species leads to the generation of UV-visible radiation; instead, the cathode and the anode during the bombardment of ions and fast electrons emit x rays, and thus, the system must be adequately shielded and chilled down.⁹

The potential difference between the negatively charged cathode and the positively charged anode accelerates the “free” electrons hitting oxygen atoms. They reduce oxygen to ROS. The low operating temperatures and the effectiveness of the electron bombardment of the gaseous oxygen mixture produce plasma-ROS rich in superoxide anions.

Then, the plasma-ROS crosses the DME device at a pressure of 1–2 bars, reaching the sampling valve or the ion-exchange semipermeable membrane filter, which blocks impurities and positively charged molecules, allowing RONS to pass to diffuse in bi-distilled water at 2–3 $\mu\text{s}/\text{cm}$. The filter, Hemoflow F5HPS, manufactured by Fresenius Medical Care AG, is an ion-exchange filter and is used as an interface between DME and the liquid. Figure 1(b) shows a schematic of the apparatus for the on-line sampling and analytical detection of the species formed during the process. Medical bi-distilled water was employed for this purpose.

B. Chemical characterization of PLO

The allotropic mixture OPL has been characterized using different methodologies:

- (i) Spectroscopic and spectrofluorimetric analysis of RONS using suitable chromophore probes.
- (ii) Ion chromatographic analysis.
- (iii) Online UV spectroscopic and conductimetric analysis.

The following probes and methods have been employed to study the reactive species present in OPL.

- (a) S36002-Singlet Oxygen Sensor Green (Life Technologies, Thermo Fisher Scientific, US). This probe is selective for the detection of singlet oxygen. Singlet Oxygen Sensor Green is specific and does not give any cross reactions with OH radicals or superoxide. The fluorescence of this probe changes

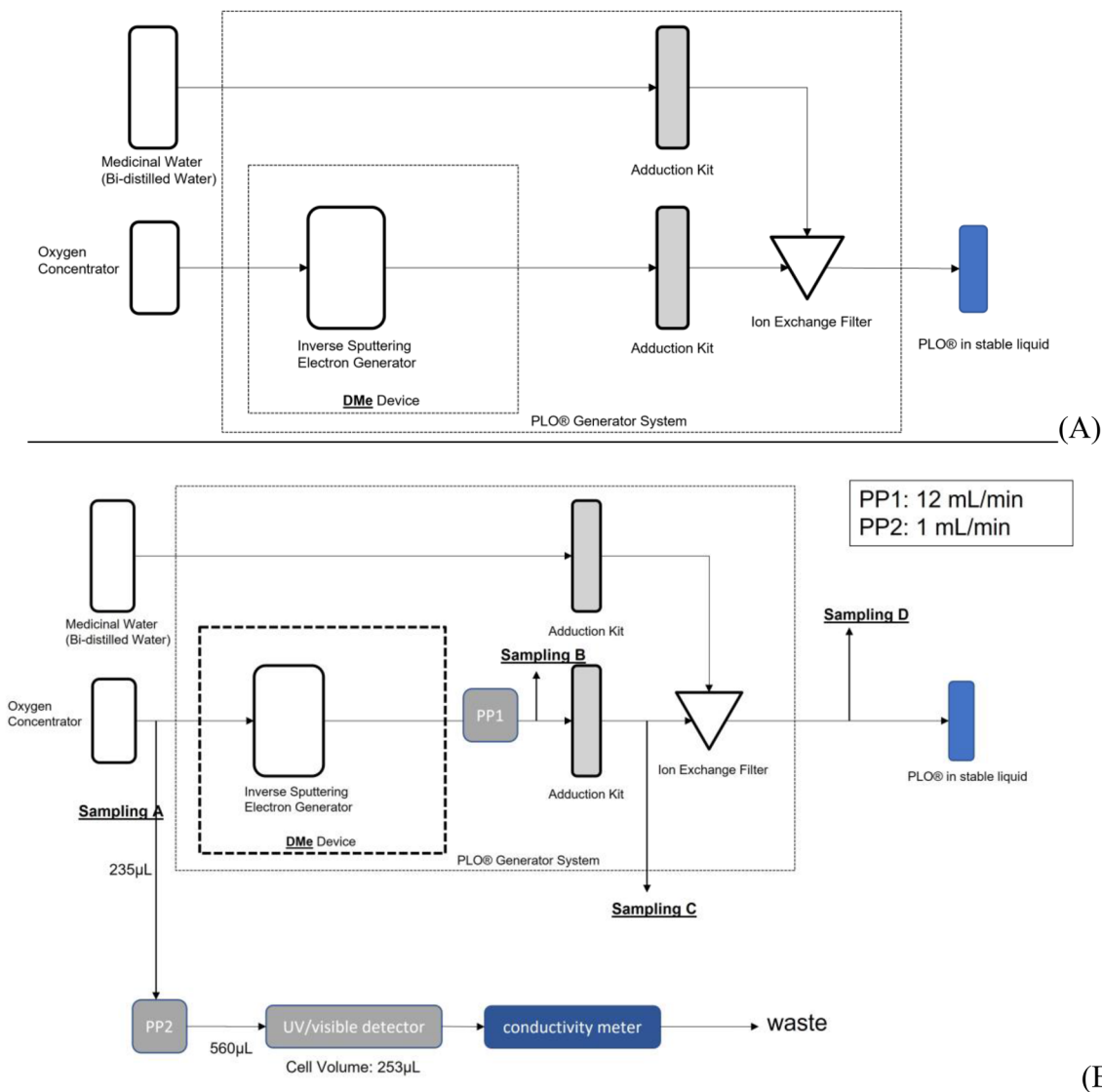


FIG. 1. (a) Schematics of the apparatus to produce PLO. (b) The apparatus has been equipped for the on-line sampling and analytical detection of the species formed during the process. PP = peristaltic pump.

from weak blue fluorescence to green in the presence of singlet oxygen ($\lambda_{\text{ex}} = 504 \text{ nm}$; $\lambda_{\text{em}} = 525 \text{ nm}$). Stock solutions were prepared in methanol, dissolving the contents of one 100 μg vial in 660 μl of methanol to make a stock solution of 250 μM . For sample/blank analysis, 10 μl of the stock solution were added in 1 ml of sample or blank (2.5 μM S36002 final concentration). The fluorescence emission spectrum was measured between 300 and 600 nm ($\lambda_{\text{ex}} = 488$ and λ_{em} maximum at 525). A Horiba FluoroMaxPLUS-TCSPC was employed for all fluorescence measurements.

- (b) D1168, dihydroethidium (3,8-phenanthridinediamine, 5-ethyl-5,6-dihydro-6-phenyl) (Life Technologies, Thermo Fisher Scientific, US), or hydroethidine, was employed for the

detection of superoxide. The stock solutions were prepared by dissolving 5 mg of D1168 in 3.17 ml of dimethyl sulfoxide (DMSO) (5 mM final concentration). An intermediate solution (IS) 500 μM was prepared in bi-distilled water. For sample/blank analysis, 40 μl of IS were added in 1 ml of sample or blank (20 μM D1168 final concentration). Emission fluorescence spectra were recorded between 300 and 700 nm ($\lambda_{\text{ex}} = 405$ and 518 nm and λ_{em} maximum at 525).

- (c) M238002, MCLA-methyl-6-(4-methoxyphenyl)-3,7-dihydroimidazo[1,2-a]pyrazin-3-one, hydrochloride (Life Technologies, Thermo Fisher Scientific, US), was employed for the detection of superoxide, emitting chemiluminescence at 455 nm. Stock solutions were prepared by dissolving

5 mg of MCLA in 3.43 ml of DMSO to get 5 mM final concentration, and 250 μM IS was prepared in bi-distilled water. For sample/blank analysis, 20 μl of the IS were added in 1 ml of sample or blank (5 μM MCLA final concentration). Chemiluminescence measurements were conducted using a spectrofluorometer in lamp off mode. The emission spectrum was also recorded between 300 and 600 nm ($\lambda_{\text{ex}} = 430$ nm and λ_{em} maximum at 549 nm).

- (d) DAF-2 (4,5-diaminofluorescein-2) (Calbiochem, La Jolla CA, USA) is a highly sensitive fluorescent probe for the detection of nitric oxide (NO). DAF-2 reacts rapidly with NO in the presence of O_2 to form the highly fluorescent triazolo-fluorescein (DAF-2T; $\lambda_{\text{ex}} = 495$ nm and $\lambda_{\text{em}} = 515$ nm). Stock solutions were prepared by dissolving 1 mg of DAF in 552 μl of DMSO to get 5 mM final concentration. A 0.5 mM IS was prepared in bi-distilled water. For sample/blank analysis, 40 μl IS were added in 1 ml of sample or blank (20 μM DAF-2 final concentration). In the presence of NO, the signal peak emission grows.
- (e) DPPH (2,2-diphenyl-1-picrylhydrazyl) (D-9132 Sigma-Aldrich Merck, Milan, Italy) was employed for antioxidant assay. DPPH has a strong visible absorption band at about 517 nm. The reduction ability of antioxidants toward DPPH is evaluated by monitoring the decrease of its absorbance at 515–528 nm as it is converted in the corresponding hydrazine DPPH₂.^{11,12} Stock solutions were prepared by dissolving 39 mg in 20 ml of methanol (5 mM final concentration). For the sample/blank analysis, 30 μl of the stock solution were added to 1.5 ml of methanol and 0.5 ml of sample or blank (75 μM DPPH final concentration). UV–vis measurements were performed using a PerkinElmer Lambda 25 UV/vis spectrophotometer in the 210–600 nm range.
- (f) Terephthalic acid (TA) (186351, Sigma-Aldrich Merck, Milan, Italy) was employed as a specific probe for hydroxyl radicals.¹³ OH radicals convert terephthalic acid to 2-hydroxyterephthalic acid (HTA, 752525 Aldrich 2-hydroxyterephthalic acid 97%) that is detected by fluorescence measurement ($\lambda_{\text{ex}} = 310$ nm and $\lambda_{\text{em}} = 425$ nm). 2 mM aqueous stock solutions of TA were prepared in 5 mM NaOH. To quantify the OH radical concentration, a calibration curve of the HTA standard solution was employed.
- (g) Cytochrome c from equine heart (C-2506, Sigma-Aldrich Merck, Milan, Italy) was employed for the detection of superoxide anions. $\text{O}_2^{\cdot-}$ reduces the ferricytochrome derivatives to ferricytochromes, which can be monitored by visible spectroscopy at 550 nm.^{14–16} This method is not specific for $\text{O}_2^{\cdot-}$, and the bimolecular rate constant for ferricytochrome reduction is only $10^6 \text{ M}^{-1} \text{ s}^{-1}$. A stock solution 416 μM ferricytochrome c was prepared by dissolving the protein powder in 0.2 mM EDTA and 50 mM phosphate buffer solution pH 8.5. A suitable volume of this solution was added to PLO solutions to get a ferricytochrome c concentration of 60 μM .

A conductimetric and UV/vis spectrophotometric detector at 240 nm ($\epsilon = 1060 \text{ M}^{-1} \text{ cm}^{-1}$) was employed for online detection of ozone.¹⁷ Ion chromatography was employed to determine the concentration of nitrite and nitrate in PLO solutions. A Dionex DX-500 ion chromatograph equipped with a GP40 gradient pump

and a Rheodyne 7125 injector (25 μl sample loop) was employed. The chromatographic separation was carried out as previously reported.¹⁸

FTIR spectroscopy (PerkinElmer Spectrum One Spectrophotometer, 32 scan averaged, 4 cm^{-1} resolution) was employed for the analysis of (i) the gas from the pleiotropic mixture generator-sputtering, (ii) the HDPE (high density polyethylene) polymeric filter employed for the active diffusion of the allotropic oxygen/nitrogen mixture into the aqueous solution.

III. RESULTS

A. In-batch experiments for the chemical characterization of PLO

1. NO, nitrite, and nitrate determination

Figure 2(a) shows the emission fluorescence spectra of DAF in PLO (curve a) compared with blank (curve b). DAF-2 reacts rapidly with NO in the presence of O_2 to form the highly fluorescent compound triazolo-fluorescein (DAF-2T; $\lambda_{\text{ex}} = 495$ nm and $\lambda_{\text{em}} = 515$ nm). The fluorescence emission at 516 nm shows that PLO contains NO radicals. Figure 2(b) shows the trend of NO radical concentration levels in PLO using various sputtering times in the gas phase.

Based on the calibration curve of DAF-2T (slope = 3.74 ± 0.14 and $R^2 = 0.9944$), we calculated that the concentration of the NO radical in PLO solutions investigated is in the 0–100 nM range, depending on the sputtering inverse time. Figure 2(b) also shows the nitrite and nitrate concentrations in PLO solutions, determined using ion chromatography. Nitrite and nitrate are the final products of NO radical oxidation.

The concentration of the NO radical decreases with the inverse sputtering electron device times, likely because of the recombination of the radical species. Nitrite/nitrate formation in the PLO solution has a trend analogous to the formation of NO radicals.

A hypothesis for the formation of NO radicals and, consequently, of nitrite and nitrate is related to the presence of water vapor in the input gas into the ozone PLO generator or to the nitrogen dissolved in water (0.014 g/l, i.e., 0.5 mM). When water vapor is present, larger quantities of nitrogen oxides are formed when sparks discharge occurs.^{19,20} Furthermore, hydroxyl radicals are formed, which are combined with oxygen radicals. All these reactions reduce the capacity of the inverse sputtering electron device.²¹ However, these molecules are essential for PLO biological activity.

2. pH, conductivity, and absorbance measurements in PLO

The pH, conductivity, and the absorbance at 258 nm of PLO solution collected in A and B sampling points [Fig. 1(b)] were measured in several batches of preliminary experiments (water flow = 1 l/h, O_2 pressure = 1 bar, 10 min inverse sputtering electron device time, and $\text{ddp} = 15.000 \text{ V}$). pH ranged between 5.1 ± 0.1 (the pH of water for injections) and 3.1 ± 0.3 . The conductivity increased from 0 up to 25–30 μS . The absorbance at 258 nm, characteristic of superoxide anions ($\epsilon = 1010 \text{ M}^{-1} \text{ cm}^{-1}$ at 260 nm),¹⁷ increased as well from 0 up to 0.1 absorbance units.

These results are consistent with the formation of superoxide anions in equilibrium with its protonated species and protons. It is

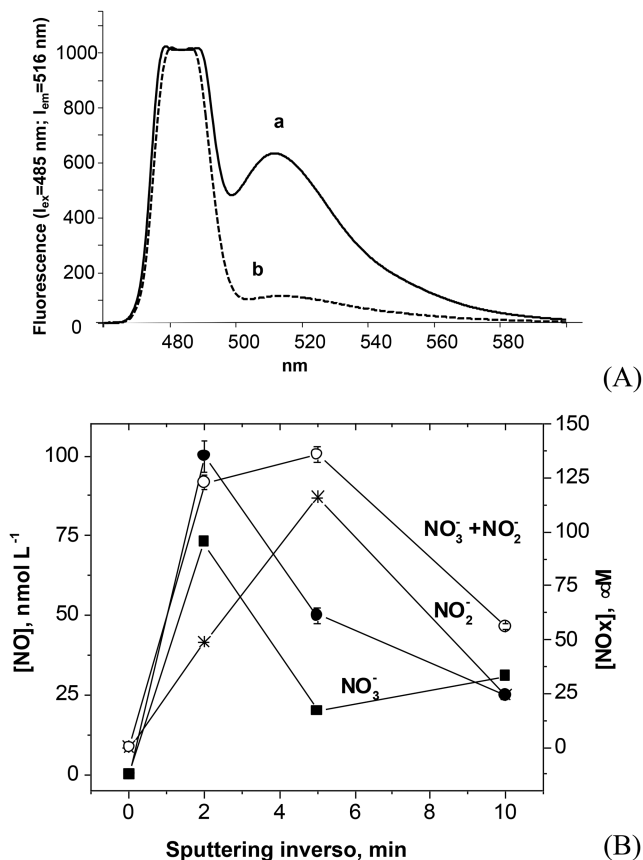


FIG. 2. (a) Emission fluorescence spectra of 400 μl PLO + 20 μl 0.5 mM DAF (a curve) compared with blank (b curve) (water flow = 1 l/h, O₂ pressure = 1 bar, ddp = 15.000 V, and 10 min inverse sputtering electron device time). (b) Concentration levels of NO (filled circles) and NO_x in PLO using various sputtering times (water flow = 1 l/h, O₂ pressure = 1 bar, and ddp = 15.000 V) (N = 3).

also known that the pK_a of the HO₃ radical is -2.1 . The presence of this species cannot be excluded.

Online measurements of pH were also performed by sampling the PLO solution in the B sampling point many times during the experiment. Figure 3 shows three representative experiments (for each sampling, the measurements were repeated N = 3 times).

B. Chemical characterization of PLO: Online measurements

1. UV absorption and conductivity

Online measurements of conductivity and absorbance at 210 nm of PLO solution were performed by sampling in A and B [Fig. 1(b)] after switching on/off the PLO generator (water flow = 1 l/h, O₂ pressure = 1 bar, 10 min inverse sputtering electron device times, [O₃] = 70 $\mu\text{g/l}$, and ddp = 15.000 V). Figure 4 shows a representative experiment with several measurements of pH [Fig. 4(a)] and online measurements [Fig. 4(b)].

The results show that UV absorbance and conductivity have analogous trends. However, UV absorbance at 210 nm shows a small

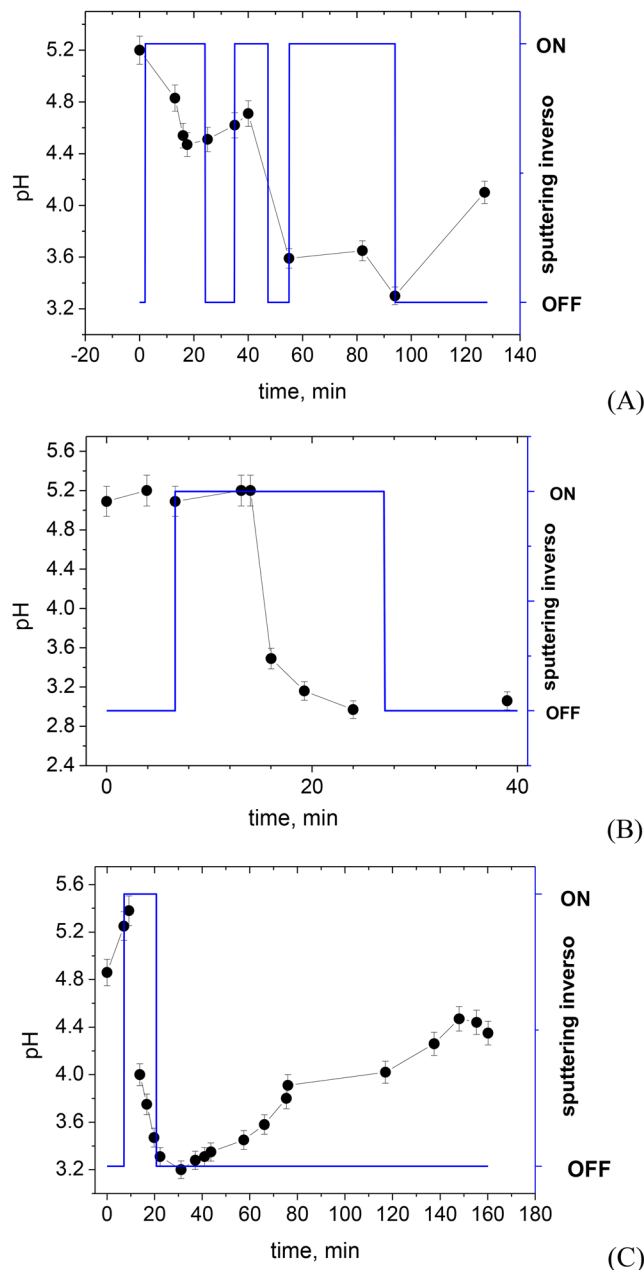


FIG. 3. Three representative experiments (A), (B), (C) in which the pH of the PLO solution sampled in B was measured (N = 3 replicates for each sampling).

increase [first arrow in Fig. 4(b)] when the inverse sputtering electron device was switched on, with a delay of about 10 min due to the dead volumes of the system. This increase takes place simultaneously to the decrease of pH observed also in the experiments of Figs. 3 and 4(a). A second larger increase in the UV signal [second arrow in Fig. 4(b)] took place simultaneously to a large increase in conductivity that started about 20–25 after switching on the inverse sputtering electron device. In correspondence with this second increase

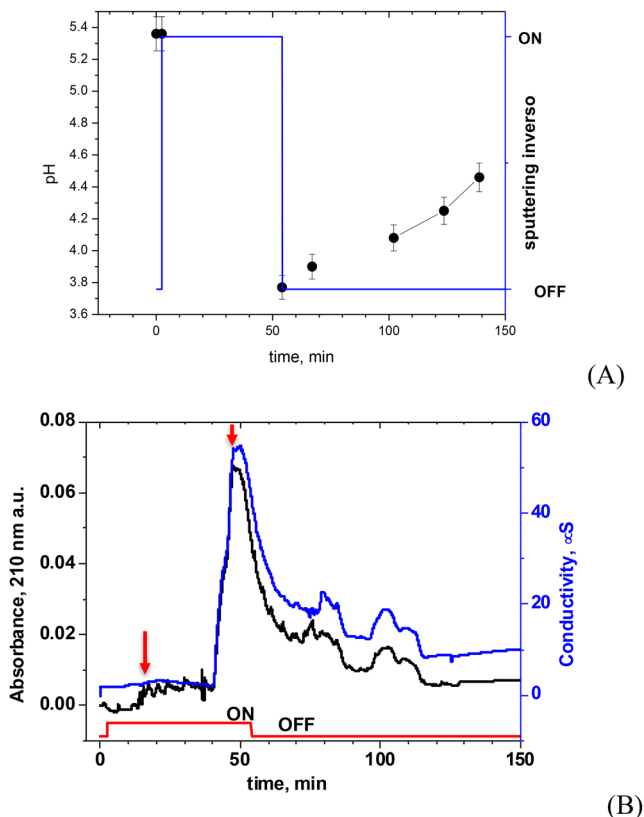


FIG. 4. (a) Trend of pH during the experiment after switching on/off the PLO generator (water flow = 1 l/h, O_2 pressure = 1 bar, 10 min inverse sputtering electron device time, and ddp = 15.000 V). (b) Online measurements of conductivity and absorbance at 210 nm of PLO solution sampled.

in the UV signal and conductivity, the pH decreased to about 3 [Fig. 4(a)].

We can hypothesize the evolution of the first radical species formed toward more absorbing species, as well as the exponential increase in the UV absorbing species.

The inverse sputtering electron device was operated for about 50 min, and then, it was switched off. After this, the UV signal and conductivity decreased slowly, never reaching the starting value in the interval observed. The pH started to re-increase slowly, as well.

2. Assay of terephthalic acid (TA) for the determination of OH radical

In order to measure the OH radicals dissolved in PLO solution, we used chemical dosimetry²² based on terephthalic acid (TA). TA is a well-known OH scavenger, which does not react with other radicals or compounds, such as O_2^- , HO_2 , and H_2O_2 . The OH radical converts TA into 2-hydroxy terephthalic acid (HTA) through the reaction shown in Fig. 5. HTA can be detected by fluorescence measurements.

Based on the experiments described in the previous paragraph, we tested three PLO solutions sampled in B: (a) 30 min after switching ON the PLO generator, (b) 30 min after switching OFF the PLO generator, and (c) 24 h after switching OFF the PLO generator

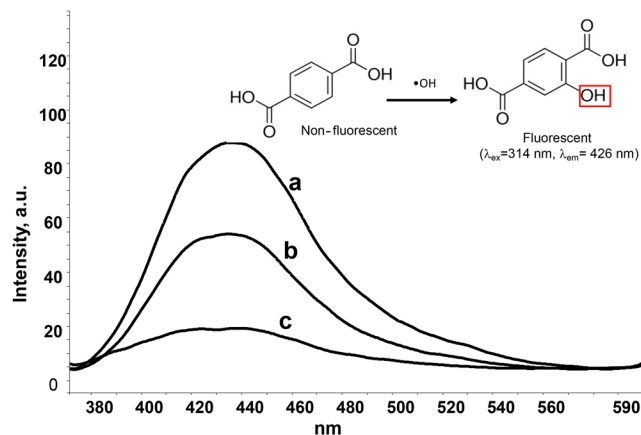


FIG. 5. Fluorescence spectrum of the PLO solutions analyzed: (a) 30 min after switching ON the PLO generator, (b) 30 min after switching OFF the PLO generator, and (c) 24 h after switching OFF the PLO generator.

(Fig. 5). The fluorescence intensity corresponds to a time integrated OH radical concentration in the liquid. Based on the fluorescence intensity at 426 nm and the calibration curve of HTA, we calculated the approximate OH radical concentration in the PLO solutions shown in Fig. 5: 6.7×10^{-6} (a), 4.2×10^{-6} (b), and 2.2×10^{-6} M (c). Other collateral reactions that compete with TA for OH radicals cannot be excluded.

3. Assay of cytochrome C for the determination of superoxide anion

Ferricytochrome c reduction assay is a classical method for detecting the rates of superoxide formation by enzymes, cells, and tissues. Superoxide reduces Ferricytochrome c (Fe^{3+} -cytochrome c) to ferricytochrome c (Fe^{2+} -cytochrome c), and the reaction rate constant is estimated to be $\sim 3 \times 10^5 \text{ M}^{-1} \text{ s}^{-1}$ at a physiologically relevant pH and room temperature.²² The reaction was monitored spectrophotometrically at 550 nm,

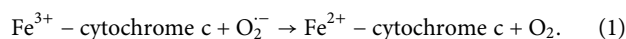


Figure 6 shows representative UV-visible spectra of the PLO solution obtained 30 min after switching ON the PLO generator (solution a) during the reaction with ferricytochrome c ($t = 0, 5, 10,$ and 15 min).

The extinction coefficient for ferricytochrome c is $0.89 \times 10^4 \text{ M}^{-1} \text{ cm}^{-1}$, and for ferricytochrome c, it is $2.99 \times 10^4 \text{ M}^{-1} \text{ cm}^{-1}$. Hence, $\Delta\epsilon$ at 550 = $2.1 \times 10^4 \text{ M}^{-1} \text{ cm}^{-1}$ is used to calculate the amount of ferricytochrome c formation in the reaction and, consequently, the concentration of superoxide anions in the PLO solution after 30 min reaction.²³ In the three PLO solutions described in the previous paragraph, the concentration of superoxide anions was 0.48, 0.57, and 0.16 μM in (a)–(c) solutions, respectively.

4. DPPH antioxidant assay and detection of superoxide anion and singlet oxygen

Figure 7 shows representative UV and fluorescence emission spectra of blank and PLO solutions spiked with DPPH for the

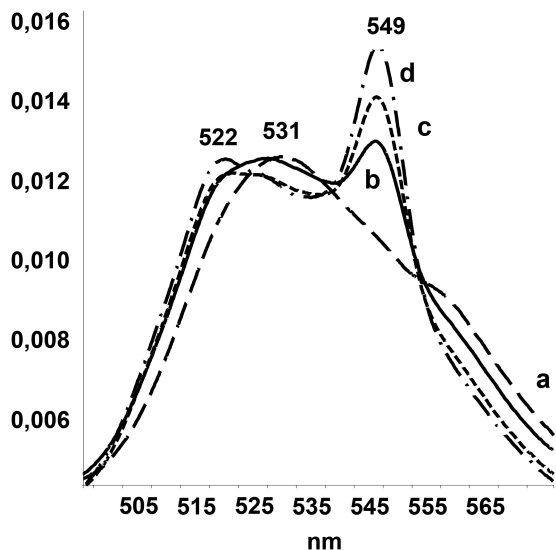


FIG. 6. Representative UV-visible spectra of the PLO solution obtained 30 min after switching ON the PLO generator (solution a) during the reaction with ferricytochrome c [t = 0 (a), 5 (b), 10 (c), and 15 min (d curve)].

detection of antioxidant radicals (a), S36002 Singlet Oxygen Sensor Green probe for the detection of singlet oxygen (b), and D1168 for the detection of superoxide anions with excitation wavelength at 405 nm (c) and 513 nm (d).

The representative results of Fig. 7(a) confirm that the PLO solution contains radical species, among these are NO, OH, and superoxide radicals. The results of Figs. 7(c) and 7(d) (insets) confirm the presence of the superoxide anion detected with the S1168 probe. Figure 7(d) shows in the PLO solution the disappearance of an emission peak at 426 nm ($\lambda_{\text{ex}} = 513$ nm) present in blank solution. The results of Fig. 7(c) also confirm the presence of singlet oxygen. These measurements are only qualitative. The concentration of each species may vary depending on the operating conditions employed to produce the PLO solution.

C. Effect of PLO solution on polymers: FTIR analysis of high density polyethylene (HDPE) films

The results of this study evidenced the presence of several radical species in PLO solutions. Thus, the oxidating power of PLO may, in principle, have multiple applications not only in life sciences but also for the treatment of materials. Here, the effect of PLO solutions on high density polyethylene (HDPE) is reported. This

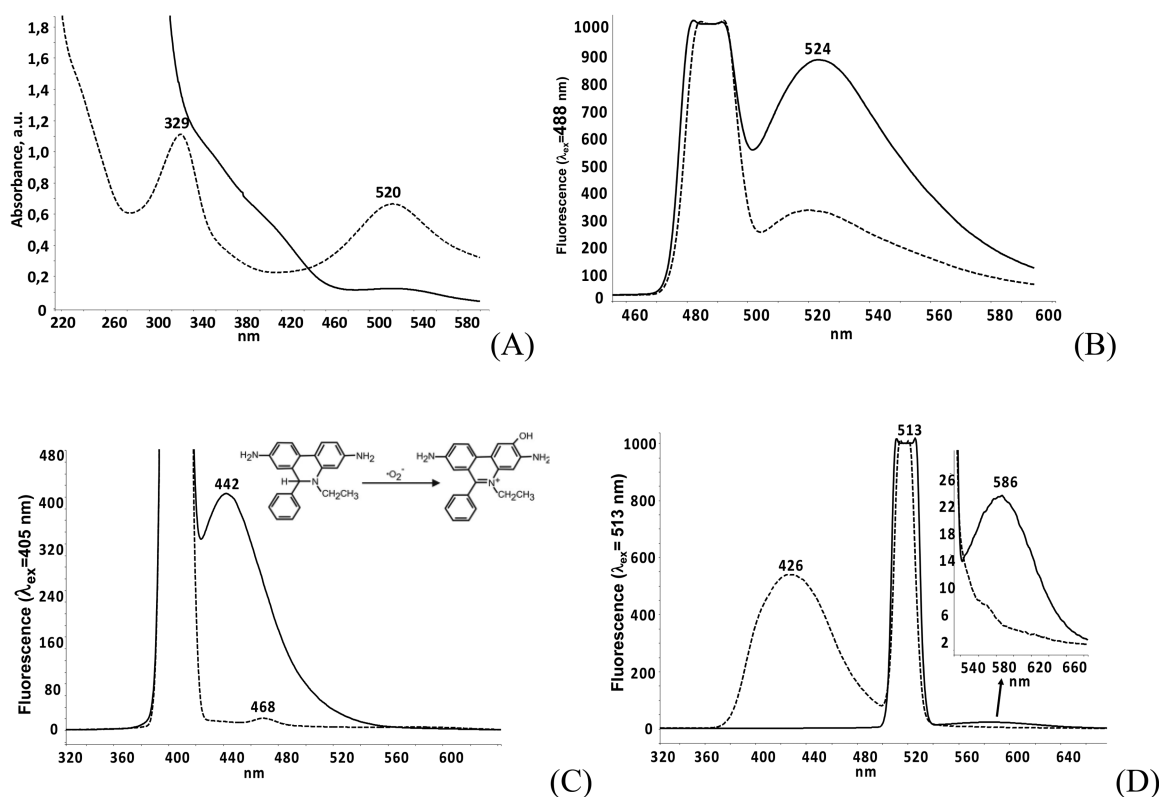


FIG. 7. Representative UV and fluorescence emission spectra of blank and PLO solutions spiked with DPPH for the detection of antioxidant radicals (a), S36002 Singlet Oxygen Sensor Green probe for the detection of singlet oxygen (b), and D1168 for the detection of superoxide anions with excitation wavelength at 405 nm (c) and 513 nm (d).

approach could be important for the surface functionalization of polymers.²⁴

After rinsing in acetone to clean the surface, HDPE films were analyzed before and after incubation for 3 days with the PLO solution sampled in the O₃ generator at the maximum value of conductivity and absorbance at 210 nm. Figure 8 shows representative FTIR spectra of HDPE films before and after PLO treatment.

The main changes in the FTIR spectra upon oxidation of polyethylene films involved in the increase in the absorbance in the 1400–1180 cm⁻¹ region associated with –C–O–C vibrations and in the region from 800 to 1100 cm⁻¹ mostly related to unsaturated C=C groups and to the formation of ozonide.

To demonstrate the formation of ozonide, the HDPE treated with the PLO solution was incubated in 0.1M HCl for 20 min in an ultrasound bath. Figure 8(b) shows representative FTIR spectra of PLO-treated HDPE films before and after the incubation in

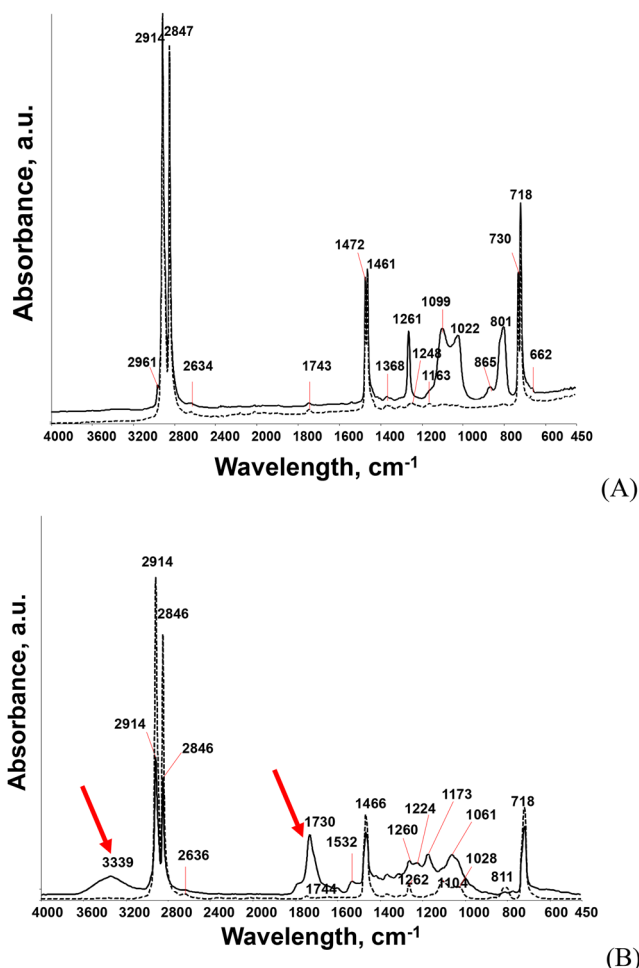


FIG. 8. (a) Representative FTIR spectra of HDPE films before (dotted line) and after (solid line) treatment with the PLO solution. (b) Representative FTIR spectra of PLO-treated HDPE films before (dotted line) and after (solid line) incubation in 0.1M HCl.

TABLE I. Radical species found in PLO solutions obtained under operating conditions optimized for this study (water flow = 1 l/h, O₂ pressure = 1 bar, ddp = 15.000 V, and 2–10 min inverse sputtering electron device time).

PLO-RONS ^(b)	Concentration (μM)
NO [•]	0.03–0.1
NO _x	25–130
•OH	2–7
O ₂ ^{•-}	0.5 ^a
Antioxidants (DPPH)	Present
Singlet oxygen	Present

^a30 min inverse sputtering electron device time was switched on.

0.1M HCl. The FTIR spectrum shows a clear formation of carboxylic compounds due to the breaking of ozonide rings.

Table I summarizes the radical species found in PLO solutions obtained under conditions optimized for this study.

IV. CONCLUSIONS

A novel methodology to produce ROS and RNS is reported. The chemical characterization of PLO-RONS reported in this work clearly shows that PLO solutions contain RONS: superoxide radical anion (O₂^{•-}), OH[•] radicals, singlet oxygen, NO radical, and H₂O₂. In the conditions explored, we found NO radical 0.03–0.1 μM, NO_x 25–130 μM, OH radical 2–7 μM, and O₂^{•-} 0.5 μM. The concentration of each species can be modulated and depends on different factors, such as inverse sputtering electron device flow rate, corona discharge parameters, water flow rate, and storage time after PLO production. PLO solutions may modify the polymer surface. In this work, we have investigated high density polyethylene, finding that this approach may be suitable for the surface functionalization of polymers. The modulation of these parameters changes the biological properties of the PLO solution, and it makes it versatile for different clinical and biotechnological applications. Based on preliminary experiments, the aqueous RONS mixtures for medical use are those rich in superoxide anion (O₂^{•-}).

AUTHOR DECLARATIONS

Conflict of Interest

The authors have no conflicts of interest to declare. All co-authors have seen and agree with the contents of the manuscript and there is no financial interest to report. We certify that the submission is original work and is not under review at any other publication.

DATA AVAILABILITY

The data that support the findings of this study are available from the corresponding author upon reasonable request.

REFERENCES

- T. Finkel, *Curr. Opin. Cell Biol.* **10**, 248 (1998).
- A. Schrammel, S. Pfeiffer, K. Schmidt, D. Koesling, and B. Mayer, *Mol. Pharmacol.* **54**, 207 (1998).
- M. C. R. Symons, *Nature* **325**, 659 (1987).
- M. D. Jyothi and A. Khar, *Nitric Oxide* **3**, 409 (1999).

- ⁵L. M. Dorfman, and G. E. Adams, NSRDS (1973).
- ⁶D. G. You, V. G. Deepagan, W. Um, S. Jeon, S. Son, H. Chang, H. I. Yoon, Y. W. Cho, M. Swierczewska, S. Lee, M. G. Pomper, I. C. Kwon, K. Kim, and J. H. Park, *Sci. Rep.* **6**, 23200 (2016).
- ⁷G. Barco, International Patent WO/2019/077391 (n.d.).
- ⁸G. K. Wehner and G. S. Anderson, in *Handbook of Thin Film Technology*, edited by L. I. Maissel and R. Glang (McGraw-Hil, New York, 1970).
- ⁹E. Nasser, *Fundamentals of Gaseous Ionization and Plasma Electronics*, Wiley-Interscience, New York (1971).
- ¹⁰N. Patron, *Trattamenti di Superficie per l'Industria* (Università degli Studi di Padova, 2005).
- ¹¹K. Pyrzynska and A. Pękal, *Anal. Methods* **5**, 4288 (2013).
- ¹²O. P. Sharma and T. K. Bhat, *Food Chem.* **113**, 1202 (2009).
- ¹³J. C. Barreto, G. S. Smith, N. H. Strobel, P. A. McQuillin, and T. A. Miller, *Life Sci.* **56**, PL89 (1995).
- ¹⁴M. G. Simic, I. A. Taub, J. Tocci, and P. A. Hurwitz, *Biochem. Biophys. Res. Commun.* **62**, 161 (1975).
- ¹⁵A. Azzi, C. Montecucco, and C. Richter, *Biochem. Biophys. Res. Commun.* **65**, 597 (1975).
- ¹⁶J. M. McCord and I. Fridovich, *J. Biol. Chem.* **244**, 6049 (1969).
- ¹⁷G. Czapski and L. M. Dorfman, *J. Phys. Chem.* **68**, 1169 (1964).
- ¹⁸B. Campanella, M. Onor, and E. Pagliano, *Anal. Chim. Acta* **980**, 33 (2017).
- ¹⁹R. Navarro-González, M. Villagrán-Muniz, H. Sobral, L. T. Molina, and M. J. Molina, *Geophys. Res. Lett.* **28**, 3867, <https://doi.org/10.1029/2001gl013170> (2001).
- ²⁰U. Schumann and H. Huntrieser, *Atmos. Chem. Phys.* **7**, 3823 (2007).
- ²¹M. A. Malik, C. Jiang, R. Heller, J. Lane, D. Hughes, and K. H. Schoenbach, *Chem. Eng. J.* **283**, 631 (2016).
- ²²Zijian Zhou *et al.*, "Reactive oxygen species generating systems meeting challenges of photodynamic cancer therapy," *Chemical Society Reviews* **1**, S91 (2016).
- ²³B. F. Van Gelder and E. C. Slater, *Biochim. Biophys. Acta* **58**, 593 (1962).
- ²⁴D. Hetemi and J. Pinson, *Chem. Soc. Rev.* **46**, 5701 (2017).